Electrical Power and Energy Systems 99 (2018) 744–755

Contents lists available at ScienceDirect

Electrical Power and Energy Systems

journal homepage: www.elsevier.com/locate/ijepes

Linear method for steady-state analysis of radial distribution systems

Anna Rita Di Fazio[a,*], Mario Russo[a], Sara Valeri[a], Michele De Santis[b]

[a] Dipartimento di Ingegneria Elettrica e dell'Informazione, Università di Cassino e del Lazio Meridionale, Cassino, Italy
[b] Engineering Department, Università Niccolò Cusano, Rome, Italy

ARTICLE INFO

Keywords:
Power system modeling
Distributed energy resources
Power distribution
Sensitivity analysis

ABSTRACT

Linear methods for steady-state analysis of distribution systems are getting more and more important due to the spreading of distributed energy resources, such as distributed generation, storage systems, active demand. This paper proposes a new linear method based on a Jacobian approach for radial distribution network with lateral derivations and distributed energy resources. The set of the linear equations modeling the distribution system is firstly presented and, then, solved in a closed form. It includes the full π-model for lines, ZIP model for uncontrolled loads, both P-Q and P-V control for distributed energy resources. The adoption of a peculiar set of modeling variables and the radial topology of the network allows to obtain high accuracy and low computational times. The effectiveness of the method is tested on both a 24-nodes and a 237-nodes network. The method is firstly applied to sensitivity analysis and compared with other linearized methods in terms of accuracy and computational efficiency; then, it is applied to the power flow analysis and compared with the classical non linear load flow.

1. Introduction

Linear methods for analyzing steady-state operation of distribution systems are gaining more and more importance in the planning and operation activities, due to the wide and rapid spread of distributed energy resources (DERs) (i.e. distributed generation, storage systems, active demand). Typical applications of linear methods are power flow analysis [1–3], power system optimization studies [4,5], power losses estimation [6], and sensitivity analysis for hosting capacity evaluation [7], for pricing and placement of DERs and control devices [8,9], for Volt/VAr control [10,11].

A widely-used approach in linear methods is to evaluate a given initial operating condition of the distribution system and, then, the sensitivity coefficients that linearly relate the variations of network electrical variables to parameter changes (i.e. powers injected by distributed generators, power exchanges by storage systems and by voltage control devices). In the present paper, this approach is adopted and attention is focused only on the impact of active and reactive powers injected/absorbed by DERs on the electrical variables of the network.

The initial operating condition is generally obtained by solving a single load-flow problem in a base-case [12]. On the other hand, several methods have been proposed to evaluate sensitivity coefficients, which can be classified into three main categories: perturb and observe methods, circuit theory methods and Jacobian-based methods.

Perturb and observe methods evaluate the sensitivity coefficients as numerical derivatives, that is the ratio between the finite variation of an electrical variable (observation) caused by an assigned DER power variation (perturbation). The variations are evaluated by either simulation [9] or actual measurements [13,14] or load-flow calculation [15,16]. Accuracy of these methods are strictly dependent on the evaluation technique (f.i. high for load-flow and low for measurements), whereas the computational efficiency is quite low if many DERs are to be considered.

The second category includes the circuit theory methods which derive the sensitivity coefficients from linear circuit equations, such as the network impedance matrix [10,15,17,18], the line voltage drop expression [11], the two-port network equations [19], the adjoint network [20]. These methods present a trade-off between accuracy of the results and computational efficiency, because the latter one can be improved only by introducing model approximations and, consequently, reducing accuracy.

The third category includes the Jacobian-based methods which, in their classical formulation, obtain the sensitivity coefficients from the inverse of the Jacobian matrix, derived from the load-flow solution [4,8]. Since these methods use the analytical derivatives, they are the most accurate but, on the other hand, present two main drawbacks: *i.* the Jacobian matrix is available from the load-flow solution obtained by the Newton-Raphson technique, which presents well-known convergence problems in distribution systems; *ii.* the computational efficiency significantly decreases with the increase of the number of the

* Corresponding author.
E-mail address: a.difazio@unicas.it (A.R. Di Fazio).

https://doi.org/10.1016/j.ijepes.2018.02.001
Received 6 November 2017; Received in revised form 18 January 2018; Accepted 1 February 2018

Nomenclature

P_{MV},Q_{MV}	powers injected by the MV voltage source
P_{LV},Q_{LV}	powers in-flowing LV busbars
P_n,Q_n	powers out-flowing the node n
P_n^{in},Q_n^{in}	powers in-flowing series parameters of the π-model of the line n
P_n^{out},Q_n^{out}	powers out-flowing series parameters of the π-model of the line n
P_n^{line},Q_n^{line}	powers out-flowing the line n
P_n^{load},Q_n^{load}	power consumptions at the node n
P_n^{der},Q_n^{der}	powers injected by DERs at the node n
P_n^{lat},Q_n^{lat}	powers flowing into the lateral derived from the node n
V_{MV}^2	square voltage at the MV busbars
V_{LV}^2	square voltage at the LV busbars
V_n^2	square voltage amplitude at the node n

nodes in the network, due to the Jacobian matrix inversion. To overcome the first drawback, in [16] the analytical derivatives are derived from the Distflow equations [21] exploiting the radial topology of distribution networks. However, the method in [16] does not overcome the second drawback. In fact, for each DER power variation, the related sensitivity coefficients are evaluated by solving a large set of linear equations.

In the present paper, extending and improving the approach presented in [22], a novel Jacobian-based method for the steady-state analysis of distribution systems is proposed by exploiting the radial network configuration, typically adopted in distribution system operation. Starting from an initial operating point, the proposed method directly provides the closed-form analytical expressions of the sensitivity coefficients, which linearly relate the variations of the active and reactive power flows and of the square nodal voltage amplitudes to the powers injected/absorbed by each DER connected to the network.

The main contributions of the paper are: (i) the model of the basic element, namely the line-node component (LNC), is extended to account for the full π-model of lines, for voltage-dependent load models, for different types of DER controls, and for lateral derivations; (ii) the set of the equations representing the linear model of the whole distribution system is provided, in which the adoption of a new set of variables for the analytical derivatives assures an improvement of the accuracy of the results with respect to other Jacobian-based methods; (iii) the closed form solution of the low-voltage (LV) distribution system is derived increasing the computational efficiency, especially for large distribution networks; (iv) the algorithm implementing the closed-form solution is outlined. The proposed model is developed with reference to balanced operating conditions, but its extension to unbalanced distribution systems is viable and will be presented in future studies.

The paper is organized as follows. In Section 2, the modeling equations of the supplying system as well as of the LV network are presented. In Section 3, the linearized model of the distribution system is firstly derived and, then, analytically solved thus obtaining its closed-form expression. Eventually, the method is firstly applied to sensitivity analysis and compared with other linearized methods in terms of accuracy and computational efficiency; then, it is applied to the power flow analysis and compared with the classical non linear load flow.

2. Distribution system modeling

Fig. 1 shows a typical LV distribution system with radial topology composed of a supplying system and the LV network. Reference is made to a LV distribution system but the analysis can be applied to medium-voltage (MV) distribution systems operating in radial configuration. Assumptions related to the modeling of the supplying system and of the LV network, which includes uncontrolled loads and DERs (i.e. photovoltaic generators, controllable loads, and storage systems), are described in the following.

2.1. Supplying system

The supplying system includes the MV distribution system and a MV/LV transformer. The former one is modeled by a voltage source imposing the no-load voltage at the MV busbar V_{MV}^2, in series with the

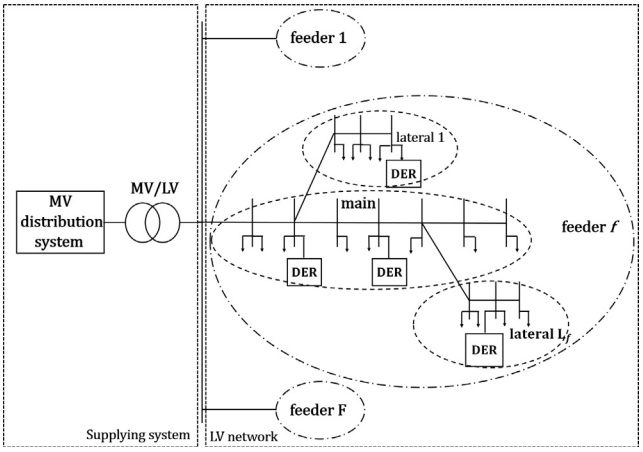

Fig. 1. Radial LV distribution system.

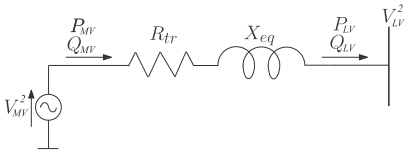

Fig. 2. Equivalent circuit of the supplying system.

short-circuit impedance X_{cc}. The transformer is modeled by its series parameters (i.e. resistance R_{tr} and leakage reactance X_{tr}). The equivalent circuit of the supplying system is shown in Fig. 2, being $X_{eq} = X_{cc} + X_{tr}$, and described by the Distflow equations [21]:

$$\begin{aligned} P_{MV} &= P_{LV} + R_{tr}\,(P_{LV}{}^2 + Q_{LV}^2)/V_{LV}^2 \\ Q_{MV} &= Q_{LV} + X_{eq}\,(P_{LV}{}^2 + Q_{LV}^2)/V_{LV}^2 \\ V_{MV}^2 &= V_{LV}^2 + 2(R_{tr}P_{LV} + X_{eq}Q_{LV}) \\ &\quad + (R_{tr}{}^2 + X_{eq}^2)(P_{LV}{}^2 + Q_{LV}^2)/V_{LV}^2 \end{aligned} \tag{1}$$

2.2. LV network

The LV network includes several feeders, each one composed of a main and different laterals. Each main and lateral is represented by a series of line-node components (LNCs). The generic nth LNC is composed of (Fig. 3): *i.* the line n between nodes $n-1$ and n; *ii.* the node n.

The line is modeled by the π equivalent circuit with series parameters (resistance R_n and reactance X_n) and shunt parameters (conductance G_n and susceptance B_n). Applying Kirchhoff laws and Distflow equations to the circuit in Fig. 3 yields:

$$\begin{aligned} P_n^{out} &= P_n^{in} - R_n\,(P_n^{in\,2} + Q_n^{in\,2})/V_{n-1}^2 \\ Q_n^{out} &= Q_n^{in} - X_n\,(P_n^{in\,2} + Q_n^{in\,2})/V_{n-1}^2 \\ V_n^2 &= V_{n-1}^2 - 2(R_n P_n^{in} + X_n Q_n^{in}) \\ &\quad + (R_n{}^2 + X_n^2)(P_n^{in\,2} + Q_n^{in\,2})/V_{n-1}^2 \end{aligned} \tag{2}$$

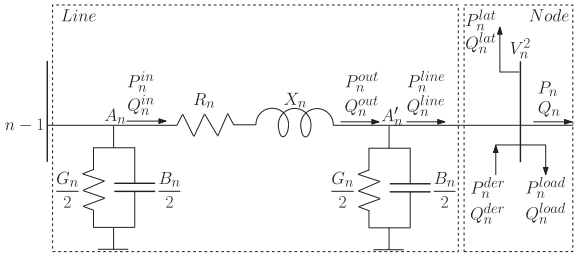

Fig. 3. Equivalent circuit of the nth LNC.

$$P_n^{in} = P_{n-1} - G_n/2\, V_{n-1}^2$$
$$Q_n^{in} = Q_{n-1} + B_n/2\, V_{n-1}^2 \tag{3}$$

$$P_n^{line} = P_n^{out} - G_n/2\, V_n^2$$
$$Q_n^{line} = Q_n^{out} + B_n/2\, V_n^2 \tag{4}$$

The node is modeled by a busbar with uncontrolled loads absorbing P_n^{load} and Q_n^{load}, DERs injecting P_n^{der} and Q_n^{der}, laterals deriving P_n^{lat} and Q_n^{lat}.

Active and reactive powers absorbed by uncontrolled loads are modeled by considering their dependence on the voltage magnitude. The ZIP model [23], widely used in distribution system studies, is adopted yielding:

$$P_n^{load} = \overline{P}_n^{load}(\gamma_n^P + \eta_n^P \sqrt{V_n^2} + \xi_n^P V_n^2)$$
$$Q_n^{load} = \overline{Q}_n^{load}(\gamma_n^Q + \eta_n^V \sqrt{V_n^2} + \xi_n^Q V_n^2) \tag{5}$$

where $\overline{P}_n^{load}$,$\overline{Q}_n^{load}$ are the rated power consumptions; γ_n^P,η_n^P,ξ_n^P are given ZIP coefficients for active power absorption; and γ_n^Q,η_n^Q,ξ_n^Q are given ZIP coefficients for reactive power absorption.

DERs can operate in a P-Q or a P-V control mode [24]. For DERs equipped with P-Q control, assigned values of active power $\overline{P}_n^{der}$ and reactive power $\overline{Q}_{\overline{n}}^{der}$ at the node n are imposed (f. i. in the case of distributed generators, $\overline{P}_n^{der}$ is the maximum power extractable from the primary energy source and $\overline{Q}_n^{der}$ can be fixed or optimally defined to offer ancillary services to the grid [25]):

$$P_n^{der} = \overline{P}_n^{der} \qquad Q_n^{der} = \overline{Q}_n^{der} \tag{6}$$

For DERs equipped with P-V control, it is assumed that the node n is connected to an additional node $\overline{n}$ by a small fictitious impedance X_n^{der}. In such a way, the P-V control imposes assigned values of active power $\overline{P}_{\overline{n}}^{der}$ and voltage $\overline{V}_{\overline{n}}^{2\,der}$ at $\overline{n}$ so that Distflow equations can be written at node n as:

$$P_n^{der} = \overline{P}_{\overline{n}}^{der}$$
$$Q_n^{der} = Q_{\overline{n}}^{der} - X_n^{der}\,(\overline{P}_{\overline{n}}^{der\,2} + Q_{\overline{n}}^{der\,2})/\overline{V}_{\overline{n}}^{2\,der}$$
$$V_n^2 = \overline{V}_{\overline{n}}^{2\,der} - 2X_n^{der} Q_{\overline{n}}^{der} + X_n^{der\,2}\,(\overline{P}_{\overline{n}}^{der\,2} + Q_{\overline{n}}^{der\,2})/\overline{V}_{\overline{n}}^{2\,der} \tag{7}$$

Finally, for notation simplicity, the powers flowing into the lateral are set equal to the dummy variables $\widetilde{P}_n^{lat}$ and $\widetilde{Q}_n^{lat}$, being determined by the lateral itself:

$$P_n^{lat} = \widetilde{P}_n^{lat} \qquad Q_n^{lat} = \widetilde{Q}_n^{lat} \tag{8}$$

3. Linear method

The proposed method aims at obtaining closed form expressions of the variations of the electrical variables characterising each node of the LV distribution network to changes of the system parameters in the same or in a different node of the grid. In the reminder, active and reactive powers absorbed by uncontrolled loads as well as active and reactive powers injected by DERs are considered as system parameters.[1]

To define variables and parameters, a rearrangement of the LNC enumeration according to the grid topology is required. For the sake of simplicity but without any loss of generality, the presence of sublaterals in the LV network is not considered to semplify the notation. In particular, as shown in Fig. 1, it is assumed that the generic feeder f ($f = 1,...,F$) is composed of a main and L_f laterals, identified by index ℓ ($\ell = 0$ for the main and $\ell = 1,...,L_F$ for the laterals). Each main and lateral is composed of $N_{f_\ell} + 1$ nodes, identified by index n ($n = 0,...,N_{f_\ell}$). The lateral ℓ is derived from a node of the main identified by the index n_{f_ℓ}. In the following variables and parameters at a generic node are indicated by three subscripts related to the feeder, the main/lateral and the node. It is worth noting that the way in which mains and laterals are identified has no impact on the method.

Variables and parameters are represented by vectors composed of active and reactive powers and the square voltage amplitude. Concerning variables, let

$$\boldsymbol{x}_{MV} = (P_{MV}, Q_{MV}, V_{MV}^2)^{\mathrm{T}}$$
$$\boldsymbol{x}_{LV} = (P_{LV}, Q_{LV}, V_{LV}^2)^{\mathrm{T}}$$
$$\boldsymbol{x}_{f,\ell,n} = (P_{f,\ell,n}, Q_{f,\ell,n}, V_{f,\ell,n}^2)^{\mathrm{T}}$$

be the vectors of the variables at the *MV* busbar, at the *LV* busbar, and at the node n of the lateral ℓ of the feeder f, respectively. Concerning parameters, let

$$\overline{\mathbf{x}}_{f,\ell,n}^{load} = (\overline{P}_{f,\ell,n}^{load}, \overline{Q}_{f,\ell,n}^{load}, 0)^{\mathrm{T}}$$
$$\overline{\mathbf{x}}_{f,\ell,n}^{der} = (\overline{P}_{f,\ell,n}^{der}, \overline{Q}_{f,\ell,n}^{der}, 0)^{\mathrm{T}}$$
$$\overline{\mathbf{x}}_{f,\ell,\overline{n}}^{der} = (\overline{P}_{f,\ell,\overline{n}}^{der}, 0, \overline{V}_{f,\ell,\overline{n}}^{2\,der})^{\mathrm{T}}$$

be the vectors of, respectively: the powers absorbed by the uncontrolled load at the node f,ℓ,n; the powers injected by DERs with P-Q control in the same node; and the active power and the voltage imposed by DERs with P-V control at the node $f,\ell,\overline{n}$. Finally, also for the lateral a vector of dummy variables is defined:

$$\widetilde{\mathbf{x}}_{f,\ell,n}^{lat} = (\widetilde{P}_{f,\ell,n}^{lat}, \widetilde{Q}_{f,\ell,n}^{lat}, 0)^{\mathrm{T}}$$

In the following, non linear equations of the distribution system model are linearized around an initial operating point; border constraints and coupling equations are added to derive the linearized model of the whole distribution system. Then, the model is analytically solved to obtain its closed-form expression and the related algorithm is outlined.

3.1. Linearized model

The initial operating point is evaluated by performing a based-case load flow solution of the LV distribution system without DERs. It is worthy noticing that the proposed method does not require that the load-flow solution in the initial operating point is performed by the Newton-Raphson technique: any load flow algorithm for distribution systems can be used.

The linearization is performed firstly for the supplying system, then for the LV network, and finally for the whole distribution system. Linearized equations are written in terms of variation of variables/parameters with respect to their values in the initial operating point (such latter values are indicated by the superscript 0 in the following).

3.1.1. Supplying system

Eqs. (1) are linearized yielding:

$$\Delta \boldsymbol{x}_{MV} = \mathbf{J}^{ss}|_0 \Delta \boldsymbol{x}_{LV} \tag{9}$$

[1] The inclusion of the changes of the operating conditions of the MV distribution system and of the effects of voltage regulator devices will be considered in future studies.

where $\mathbf{J}^{ss}|_0$ is Jacobian matrix. Model (9) expresses the variations of the variables of the MV distribution system $\Delta\boldsymbol{x}_{MV}$ as linear function of variation of the same variables at the LV busbar $\Delta\boldsymbol{x}_{LV}$. It is important to notice that in $\Delta\boldsymbol{x}_{MV}$:

$$\Delta V_{MV}^2 = V_{MV}^2 - V_{MV}^{0^2}$$

and, then, its value is assigned; in the following it is assumed that $\Delta V_{MV}^2 = 0$, neglecting the changes of the operating conditions of the MV distribution system.

3.1.2. LV network

The model of the LV network is represented by a set of feeder models; each feeder model is composed in turns of the main model, L_f lateral models and the coupling equations among main and laterals. Models of both main and laterals include a set of linearized equations of the LNC model, which is developed in Appendix A, and border constraints. In details:

$$\begin{aligned}
&\textit{feeder } f \quad (f = 1...,F)\\
&\quad \textit{main} \quad \ell = 0\\
&\quad \Delta\boldsymbol{x}_{f,0,n} = \mathbf{J}_{f,0,n}\Delta\boldsymbol{x}_{f,0,n-1} + \overline{\mathbf{J}}_{f,0,n}(\Delta\overline{\mathbf{x}}_{f,0,n}^{inj} - \Delta\widetilde{\mathbf{x}}_{f,0,n}^{lat})\\
&\quad \text{for } n = 1,...,N_{f_0}\\
&\quad \Delta P_{f,0,N_{f_0}} = 0 \quad \Delta Q_{f,0,N_{f_0}} = 0 \quad \Delta V_{f,0,0}^2 = \Delta V_{LV}^2
\end{aligned} \tag{10}$$

$$\begin{aligned}
&\quad \textit{laterals } \ell \quad (\ell = 1...,L_f)\\
&\quad \Delta\boldsymbol{x}_{f,\ell,n} = \mathbf{J}_{f,\ell,n}\Delta\boldsymbol{x}_{f,\ell,n-1} + \overline{\mathbf{J}}_{f,\ell,n}\Delta\overline{\mathbf{x}}_{f,\ell,n}^{inj}\\
&\quad \text{for} \quad n = 1,...,N_{f_\ell}\\
&\quad \Delta P_{f,\ell,N_{f_\ell}} = 0 \quad \Delta Q_{f,\ell,N_{f_\ell}} = 0 \quad \Delta V_{f,\ell,0}^2 = \Delta V_{f,0,n_{f_\ell}}^2
\end{aligned} \tag{11}$$

$$\begin{aligned}
&\quad \textit{coupling main and laterals}\\
&\quad \Delta\widetilde{P}_{f,0,n_{f_\ell}}^{lat} = \Delta P_{f,\ell,0} \quad \Delta\widetilde{Q}_{f,0,n_{f_\ell}}^{lat} = \Delta Q_{f,\ell,0}\\
&\quad \text{for} \quad \ell = 1,...,L_f
\end{aligned} \tag{12}$$

where $\mathbf{J}_{f,\ell,n}$ and $\overline{\mathbf{J}}_{f,\ell,n}$ are defined in Appendix A.

Equations in (10) are the linearized model of the main. The first set of equations are the N_{f_0} LCN models; each LNC model expresses the variation of the electrical variables at each node of the main $\Delta\boldsymbol{x}_{f,0,n}$ as linear function of: (i) the variation of the electrical variables at the upstream node $\Delta\boldsymbol{x}_{f,0,n-1}$; (ii) the variations of assigned absorbed/injected powers due to uncontrolled loads and DERs at the same node $\Delta\overline{\mathbf{x}}_{f,0,n}^{inj}$, defined by (33) in Appendix A; (iii) the variation of the powers flowing into the lateral $\Delta\widetilde{\mathbf{x}}_{f,0,n}^{lat}$. The second set of equations in (10) represent 3 border constraints, imposing that the active and reactive power flowing at the ending LNC of the main are null and that the variation of the voltage at the beginning of the main is equal to the one at the LV busbar.

Similarly to (10), each lateral in (11) is modeled by a set of N_{f_ℓ} LNC models (with no lateral derivation) and a set of 3 border conditions (imposing null powers at the ending nodes and the equality among the variation of the voltage at the beginning of the lateral and at the node n_{f_ℓ} of the main, which the lateral is derived from).

Finally, coupling Eqs. (12) impose that the powers flowing out of the main are equal to the ones flowing into the laterals.

It is important to notice that the presence of a lateral with sublaterals in the LV network can trivially be taken into account by writing equations similar to (10)–(12).

3.1.3. LV distribution system

The linearized model of the whole LV distribution system is composed of the model of the supplying system (9), the feeder models (10)–(12) for $f = 1,...,F$, and the coupling equations imposing the balance among the variations of the active and reactive powers outflowing the LV busbar and inflowing the feeders:

$$\Delta P_{LV} = \sum_{f=1}^{F} \Delta P_{f,0,0} \quad \Delta Q_{LV} = \sum_{f=1}^{F} \Delta Q_{f,0,0} \tag{13}$$

The adoption of the squared voltages rather than the voltage amplitudes as variables of the model allows to reduce the approximations introduced by the linearization with respect to other Jacobian methods. The set (9)–(13) can be numerically solved for assigned $\overline{\mathbf{x}}_{f,\ell,n}^{inj}$, similarly to [16]. To avoid the solution of a large linear problem, in the following the closed-form solution of the model is derived by exploiting the radial topology of the distribution system.

3.2. Closed-form solution

Applying the chain rule to the first equation of the model of the main in (10), it is induced:

$$\begin{aligned}
\Delta\boldsymbol{x}_{f,0,n} &= \mathbf{M}_{f,0,n}\Delta\boldsymbol{x}_{f,0,0}\\
&\quad + \sum_{k=1}^{N_{f_0}} \mathbf{N}_{f,0,n}(f,0,k)(\Delta\overline{\mathbf{x}}_{f,0,k}^{inj} - \Delta\widetilde{\mathbf{x}}_{f,0,k}^{lat})\\
&\text{for } n = 1,...,N_{f_0}
\end{aligned} \tag{14}$$

where $\mathbf{M}_{f,0,n}$ and $\mathbf{N}_{f,0,n}(f,0,k)$ are defined in Table 1. For assigned $\overline{\mathbf{x}}_{f,0,k}^{inj}$ and $\widetilde{\mathbf{x}}_{f,0,k}^{lat}$, (14) is a set of N_{f_0} equations in $N_{f_0} + 1$ variables, i.e. $\Delta\boldsymbol{x}_{f,0,n}$ and $\Delta\boldsymbol{x}_{f,0,0}$. Imposing the 3 border constraints in (10), the set (14) is analytically solved with respect to $\Delta\boldsymbol{x}_{f,0,n}$ with $n = 0,...,N_{f_0}$ applying the same procedure as in [22], yielding:

$$\begin{aligned}
\Delta\boldsymbol{x}_{f,0,n} &= \sum_{k=1}^{N_{f_0}} \mathbf{A}_{f,0,n}(f,0,k)\Delta\overline{\mathbf{x}}_{f,0,k}^{inj}\\
&\quad - \sum_{j=1}^{L_f} \mathbf{A}_{f,0,n}(f,0,n_{f_j})\Delta\widetilde{\mathbf{x}}_{f,0,n_{f_j}}^{lat} + \mathbf{a}_{f,0,n}\Delta V_{LV}^2\\
&\text{for } n = 0,...,N_{f_0}
\end{aligned} \tag{15}$$

where $\mathbf{A}_{f,0,n}(f,0,k)$ and $\mathbf{a}_{f,0,n}$ are defined in Table 1.

In a similar way the lateral models are derived, resulting:

Table 1
Expressions of vectors and matrices for main and laterals.

$\mathbf{M}_{f,\ell,n}$	$\mathbf{N}_{f,\ell,n}(f,\ell,k)$	$\mathbf{A}_{f,\ell,n}(f,\ell,k)$	$\mathbf{A}_{f,\ell,0}(f,\ell,k)$	$\mathbf{a}_{f,\ell,n}$	$\mathbf{a}_{f,\ell,0}$
$\prod_{h=0}^{n-1}\mathbf{J}_{f,\ell,n-h}$	$\prod_{h=0}^{n-k-1}\mathbf{J}_{f,\ell,n-h}\overline{\mathbf{J}}_{f,\ell,k} \quad k < n$ $\overline{\mathbf{J}}_{f,\ell,k} \quad k = n$ $\mathbf{0} \quad k > n$	$\mathbf{M}_{f,\ell,n}\mathbf{A}_{f,\ell,0}(f,\ell,k)$ $+ \mathbf{N}_{f,\ell,n}(f,\ell,k)$	$\begin{pmatrix} \overline{\mathbf{A}}_{f,\ell,0}(f,\ell,k) & 0 \\ & 0 \\ 0 \quad 0 & 0 \end{pmatrix}$	$\mathbf{M}_{f,\ell,n}\mathbf{a}_{f,\ell,0}$	$\begin{pmatrix} \overline{\mathbf{a}}_{f,\ell,0} \\ 1 \end{pmatrix}$

where: $\overline{\mathbf{A}}_{f,\ell,0}(f,\ell,k) = -\overline{\mathbf{M}}_{f,\ell,N_{f_\ell}}^{-1}\overline{\mathbf{N}}_{f,\ell,N_{f_\ell}}(f,\ell,k)$ $\quad$ $\overline{\mathbf{a}}_{f,\ell,0} = -\overline{\mathbf{M}}_{f,\ell,N_{f_\ell}}^{-1}\overline{\mathbf{m}}_{f,\ell,N_{f_\ell}}$

$\overline{\mathbf{M}}_{f,\ell,N_{f_\ell}}$ is the (2 × 2) principal minor of $\mathbf{M}_{f,\ell,N_{f_\ell}}$ $\quad$ $\overline{\mathbf{N}}_{f,\ell,N_{f_\ell}}(f,\ell,k)$ is the (2 × 2) principal minor of $\mathbf{N}_{f,\ell,N_{f_\ell}}(f,\ell,k)$

$\overline{\mathbf{m}}_{f,\ell,N_{f_\ell}}$ is the (2 × 1) vector with the 1st and 2nd elements of the 3rd column of $\mathbf{M}_{f,\ell,N_{f_\ell}}$.

$$\Delta \boldsymbol{x}_{f,\ell,n} = \sum_{k=1}^{N_{f\ell}} \mathbf{A}_{f,\ell,n}(f,\ell,k)\Delta\overline{\mathbf{x}}^{inj}_{f,\ell,k} + \mathbf{a}_{f,\ell,n}\Delta V^2_{f,0,n_{f\ell}}$$
$$\text{for } n = 0,\ldots,N_{f\ell} \quad \ell = 1,\ldots,L_f \tag{16}$$

where $\mathbf{A}_{f,\ell,n}(f,\ell,k)$ and $\mathbf{a}_{f,\ell,n}$ are defined in Table 1.

As demonstrated in Sect. A of the Appendix B, by imposing (12) to couple the main (15) and laterals (16) for each feeder f, it is obtained the model of the LV network as:

$$\Delta \boldsymbol{x}_{f,\ell,n} = \sum_{j=0}^{L_f}\sum_{k=1}^{N_{fj}} \mathbf{U}_{f,\ell,n}(f,j,k)\Delta\overline{\mathbf{x}}^{inj}_{f,j,k} + \mathbf{u}_{f,\ell,n}\Delta V^2_{LV}$$
$$\text{for } f = 1,\ldots,F \quad \ell = 0,\ldots,L_f \quad n = 0,\ldots,N_{f\ell} \tag{17}$$

where $\mathbf{U}_{f,\ell,n}(f,j,k)$ and $\mathbf{u}_{f,\ell,n}$ are defined in Appendix B.

It is worth underlining that the model of a lateral with sublaterals can trivially be included by writing equations similar to (15)–(17) and, for each feeder, by hierarchically coupling firstly lateral with its sublaterals and then main with its laterals.

The distribution system is represented by the model of the supplying subsystem (9) and the model of the LV network (17). As demonstrated in Sect. B of Appendix B, imposing the balance of powers (13) at the LV busbar the closed form expression of the model of the LV distribution system is obtained:

$$\Delta \boldsymbol{x}_{f,\ell,n} = \sum_{i=1}^{F}\sum_{j=0}^{L_i}\sum_{k=1}^{N_{fj}} \mathbf{T}_{f,\ell,n}(i,j,k)\Delta\overline{\mathbf{x}}^{inj}_{i,j,k}$$
$$\text{for } f = 1,\ldots,F \quad \ell = 0,\ldots,L_f \quad n = 0,\ldots,N_{f\ell} \tag{18}$$

where $\mathbf{T}_{f,\ell,n}(i,j,k)$ is defined in Appendix B. Model (18) linearly relates the variations of the electrical variables characterising each node of the LV distribution network to the variations of powers injected by all the uncontrolled loads and DERs connected to the grid. Such a model can be applied to linear modeling of the steady-state operation as well as to perform sensitivity analysis of the distribution system. As an example of the former application, the simple case of a distribution system with fixed uncontrolled loads and distributed generation with P-Q control as DERs can be considered; assuming the distribution system without DERs as initial operating point, using (18) the steady-state linear model can be rewritten as

$$\boldsymbol{x}_{f,\ell,n} = \boldsymbol{x}^0_{f,\ell,n} + \sum_{i=1}^{F}\sum_{j=0}^{L_i}\sum_{k=1}^{N_{fj}} \mathbf{T}_{f,\ell,n}(i,j,k)(P^{der}_{i,j,k}, Q^{der}_{i,j,k}, 0)^{\mathrm{T}}$$
$$\text{for } f = 1,\ldots,F \quad \ell = 0,\ldots,L_f \quad n = 0,\ldots,N_{f\ell} \tag{19}$$

In addition, model (18) can be used to perform sensitivity analysis. In fact, since the linearity of the model allows the superposition effect, it can be used to evaluate the impact of a single DER injection on the electrical variables of a specific node of the grid, according to

$$\Delta \boldsymbol{x}_{f,\ell,n} = \mathbf{T}_{f,\ell,n}(i,j,k)\Delta\overline{\mathbf{x}}^{inj}_{i,j,k} \tag{20}$$

3.3. Algorithm

A general algorithm is presented to evaluate the closed form expression of the linear model of the LV distribution system. The algorithm is divided into two procedures.

3.3.1. First procedure

The input data are:

- configuration of the distribution system;
- supplying system parameters: $V_{MV}, X_{cc}, R_{tr}, X_{tr}$;
- line parameters: R_n, X_n, G_n, B_n;
- uncontrolled load parameters: $\overline{P}^{load}_n, \overline{Q}^{load}_n, \gamma^P_n, \eta^P_n, \xi^P_n, \gamma^Q_n, \eta^Q_n, \xi^Q_n$;
- parameters of DERs with P-Q control: $\overline{P}^{der}_n, \overline{Q}^{der}_n$;
- parameters of DERs with P-V control: $\overline{P}^{der}_{\overline{n}}, \overline{V}^{der}_{\overline{n}}$;
- active and reactive power flows and voltage amplitudes in the initial operating point: $\mathbf{x}^0_n$.

Such a procedure evaluates the new arrangement of the LV network and the Jacobian matrices of the supplying system and of the LNCs. In details, it consists of:

i. rearranging the LV network in F feeders and each feeder f in a main $\ell = 0$ with $N_{f_0} + 1$ nodes and $\ell = 1,\ldots,L_F$ laterals with $N_{f\ell} + 1$ nodes;
ii. evaluating the Jacobian matrix of the supplying system $\mathbf{J}^{ss}|_0$ in (9);
iii. evaluating the Jacobian matrices for each LNC:
   - line: $\mathbf{J}^{line}_{f,\ell,n}|_0$ in (24);
   - uncontrolled load: $\mathbf{J}^{load_1}_{f,\ell,n}|_0$ and $\mathbf{J}^{load_2}_{f,\ell,n}|_0$ in Table 14;
   - DER with P-V control: $\mathbf{J}^{der_1}_{f,\ell,n}|_0$ and $\mathbf{J}^{der_2}_{f,\ell,n}|_0$ in Table 14;
   - LNC: $\mathbf{J}_{f,\ell,n}$ and $\overline{\mathbf{J}}_{f,\ell,n}$ in (34).

3.3.2. Second procedure

The input data are the output of the first procedure; in detail:

- rearrangement of the LV network;
- Jacobian matrix of the supplying system $\mathbf{J}^{ss}|_0$;
- Jacobian matrices of the LV network $\mathbf{J}_{f,\ell,n}$ and $\overline{\mathbf{J}}_{f,\ell,n}$;

Such a procedure evaluates the matrices $\mathbf{T}_{f,\ell,n}$ in (18). In detail, it consists of:

i. for each node of both main of its laterals of a feeder, evaluating matrices $\mathbf{A}_{f,\ell,n}$ and vectors $\mathbf{a}_{f,\ell,n}$ in Table 1;
ii. for each feeder, coupling main and its laterals by evaluating matrices $\mathbf{U}_{f,\ell,n}$ and vectors $\mathbf{u}_{f,\ell,n}$ in Table 15;
iii. coupling supplying substation and feeders of the LV network by evaluating matrices $\mathbf{T}_{f,\ell,n}$ in Table 16.

The second procedure is described in Fig. 4.

In conclusion, such an algorithm can be implemented in any programming language and can be included into commercial software,

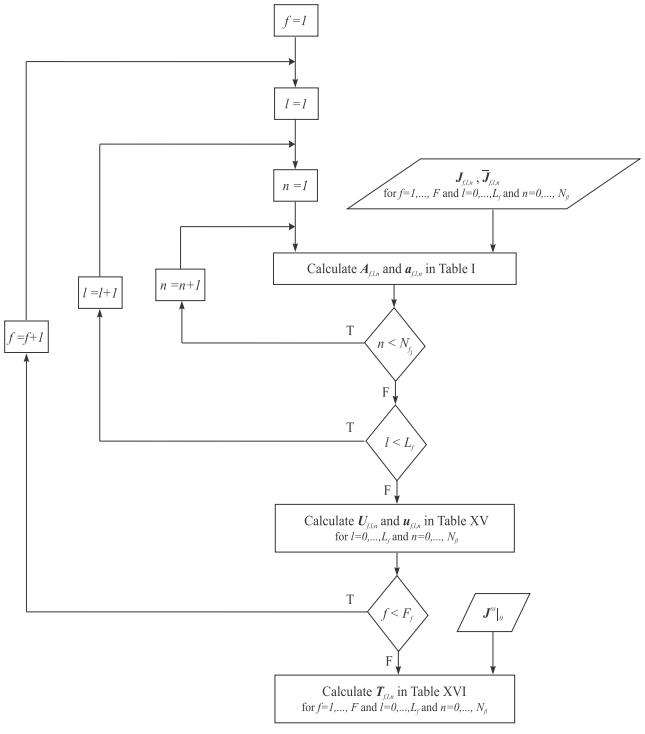

Fig. 4. Algorithm.

provided that adequate interface is implemented for the rearrangement of input and output data.

4. Case study

The proposed method (PM) is firstly applied to sensitivity analysis and compared with other methods used to evaluate sensitivity coefficients in terms of accuracy and computational times; then, it is applied to the load flow problem and compared with non-linear load flow solution.

4.1. Application to sensitivity analysis: accuracy

The PM is applied to perform sensitivity analysis and evaluate the variations of the electrical variables ΔP_n,ΔQ_n,ΔV_n caused by changes of injections/absorptions of the DERs connected to the grid.

To evaluate the accuracy of the PM, results are compared with the benchmark variations of the electrical variables $\Delta P_{ref,n}$,$\Delta Q_{ref,n}$,$\Delta V_{ref,n}$, obtained by load flow solution; in particular errors are calculated for the three electrical variable at each node as:

$$e_{P_n} = |\Delta P_n - \Delta P_{ref,n}|$$
$$e_{Q_n} = |\Delta Q_n - \Delta Q_{ref,n}|$$
$$e_{V_n} = |\Delta V_n - \Delta V_{ref,n}|.$$

The PM is compared with other two sensitivity-based methods: the circuit theory method (CTM), based on network impedance matrix presented in [18], and the classical Jacobian method (JM), based on the inverse of the Jacobian matrix. The accuracy of both CTM and JM is evaluated in the same way.

In the following the results for two distribution systems are analyzed, namely a 24-nodes and a 237-nodes LV networks.

4.1.1. 24-nodes LV network

A 20/0.4 kV substation feeds a LV distribution grid composed of 2 main feeders, each one with 2 laterals and 2 DERs (Fig. 5). The 20 kV distribution system is represented by its Thevenin equivalent as seen from the MV/LV substation, assuming a 1000 MVA short-circuit power and an open-circuit voltage $V_{MV} = 1.0$ p.u.. Concerning the 20/0.4 kV transformer, it has a rated power equal to 0.25 MVA with $X_{tr} = 0.015$ p.u. and $R_{tr} = 0.00125$ p.u.. The electrical parameters of the lines and the rated powers absorbed by uncontrolled loads are reported in Table 2. Hereafter the basis is set to 100 kVA. The total load connected to the network is equal to 65.9 kW and 33.0 kVAr. In the following, both small and large DER injections/absorptions are taken into account to test the accuracy of the linearization.

Small DER powers. Two different cases are considered to take into account power injections and absorptions of DERs:

(1) 4 DERs of PQ-type, each one injecting $\overline{P}^{der} = 3$ kW and $\overline{Q}^{der} = 1.5$ kVAr; uncontrolled loads of PQ-type;
(2) 4 DERs of PQ-type, each one absorbing $\overline{P}^{der} = -3$ kW and $\overline{Q}^{der} = -1.5$ kVAr; uncontrolled loads of PQ-type;

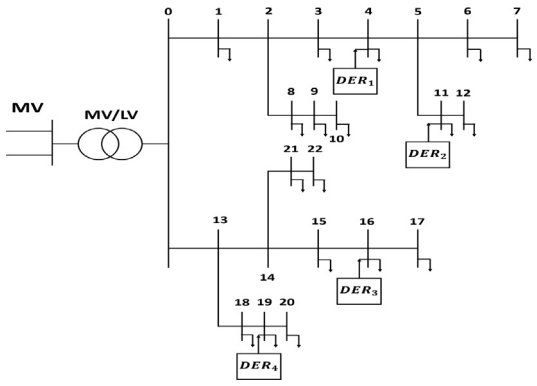

Fig. 5. 24-nodes LV network.

Table 2
Line and load parameters for the 24-nodes LV network.

From Node	To Node	R (p.u.)	X (p.u.)	$\overline{P}^{load}$ (p.u.)	$\overline{Q}^{load}$ (p.u.)
0	1	0.0105	0.0025	0.0261	0.0128
1	2	0.0059	0.0014	0.0236	0.0117
2	3	0.0114	0.0027	0.0152	0.0075
3	4	0.0079	0.0011	0.0138	0.0068
4	5	0.0095	0.0013	0.0124	0.0062
5	6	0.0052	0.0007	0.0033	0.0016
6	7	0.0040	0.0006	0.0020	0.0010
2	8	0.0106	0.0015	0.0062	0.0031
8	9	0.0120	0.0017	0.0041	0.0020
9	10	0.0040	0.0006	0.0020	0.0010
5	11	0.0089	0.0011	0.0040	0.0020
11	12	0.0037	0.0002	0.0020	0.0010
0	13	0.0006	0.0001	0.0373	0.0183
13	14	0.0190	0.0010	0.0228	0.0111
14	15	0.0100	0.0005	0.0093	0.0046
15	16	0.0088	0.0004	0.0041	0.0020
16	17	0.0408	0.0019	0.0020	0.0010
13	18	0.0038	0.0008	0.0122	0.0060
18	19	0.0512	0.0027	0.0067	0.0033
19	20	0.0236	0.0012	0.0014	0.0007
14	21	0.0632	0.0096	0.0065	0.0032
21	22	0.0017	0.0003	0.0013	0.0006

Tables 3 and 4 reports the average and the maximum values of the errors for the three methods PM, JM and CTM in the cases 1 and 2, respectively. Both the tables show that CTM presents errors of at least one order of magnitude larger than PM and JM. For this reason, CTM is no longer taken into consideration in the following. Furthermore, PM and JM present errors of the same order of magnitude and in any case PM gives better results than JM. Comparing Table 3 with Table 4 it is apparent that the corresponding errors are very similar and consequently in the following only DER power injections are analyzed.

Large DER powers. Three different cases are considered, to take into account different types of control for DERs and of uncontrolled loads:

Table 3
Errors for the 24-nodes network: case 1.

	Average error [10^{-3} p.u.]			Maximum error [10^{-3} p.u.]		
	P	Q	V	P	Q	V
PM	0.0045	0.0006	0.0576	0.0233	0.0048	0.0988
JM	0.0077	0.0040	0.0988	0.0257	0.0162	0.2135
CTM	0.0584	0.0417	0.9348	0.1960	0.1480	1.7783

Table 4
Errors for the 24-nodes network: case 2.

	Average error [10^{-3} p.u.]			Maximum error [10^{-3} p.u.]		
	P	Q	V	P	Q	V
PM	0.0047	0.0007	0.0621	0.0247	0.0051	0.1082
JM	0.0080	0.0040	0.1043	0.0271	0.0162	0.2266
CTM	0.1470	0.0982	2.3077	0.4450	0.2881	3.9062

Table 5
Errors for the 24-nodes network: case 3.

	Average error [10^{-3} p.u.]			Maximum error [10^{-3} p.u.]		
	P	Q	V	P	Q	V
PM	0.1767	0.0250	2.1253	0.8937	0.1865	3.5174
JM	0.3184	0.1773	3.8430	1.0021	0.7351	8.2168

Table 6
Errors for the 24-nodes network: case 4.

	Average error [10^{-3} p.u.]			Maximum error [10^{-3} p.u.]		
	P	Q	V	P	Q	V
PM	0.2738	0.4282	0.3953	1.2913	1.8620	1.7689
JM	0.3103	0.6307	0.7819	1.1258	3.3187	2.3171

Table 7
Errors for the 24-nodes network: case 5.

	Average error [10^{-3} p.u.]			Maximum error [10^{-3} p.u.]		
	P	Q	V	P	Q	V
PM	0.1480	0.0180	1.7114	0.7267	0.1414	2.7925
JM	0.2687	0.1472	3.1653	0.8173	0.6168	6.7703

(3) 4 DERs of PQ-type, each one injecting $\overline{P}^{der} = 20$ kW and $\overline{Q}^{der} = 10$ kVAr; uncontrolled loads of PQ-type;
(4) DER_1, DER_3 of PV-type (with voltage set to 1.0 p.u.), each one injecting $\overline{P}^{der} = 20$ kW; DER_2, DER_4 of PQ-type, each one injecting $\overline{P}^{der} = 20$ kW and $\overline{Q}^{der} = 10$ kVAr; uncontrolled loads of PQ-type;
(5) 4 DERs of PQ-type, each one injecting $\overline{P}^{der} = 20$ kW and $\overline{Q}^{der} = 10$ kVAr; uncontrolled loads of ZIP-type with $\gamma_n^P = \eta_n^P = \gamma_n^Q = \eta_n^Q = 0$ and $\xi_n^P = \xi_n^Q = 1$;

The results for the cases 3, 4 and 5 are reported in Tables 5–7, respectively. In all the cases, PM assures higher accuracy than JM with the only exception of the maximum error on P in the case 4.

4.1.2. 237-nodes network

The LV distribution grid is obtained by adding to the previous 24-nodes LV network a third feeder described in the IEEE European LV test network [26]; the resulting LV network is composed of 237 nodes and presents multiple laterals derived from both mains and other laterals. The total load connected to the network is equal to 108.3 kW and 46.9 kVAr. Eleven DERs are connected to the grid (3 DERs to the first feeder, 3 DERs to the second feeder and 5 DERs to the third feeder). Each DER injects $\overline{P}^{der} = 10$ kW and $\overline{Q}^{der} = 5$ kVAr. Three different cases are considered:

(1) DERs and uncontrolled loads of PQ-type;
(2) 3 DERs of PV-type (with voltage set to 1.0 p.u.) and 8 DERs of PQ-type; uncontrolled loads of PQ-type;
(3) DERs of PQ-type; uncontrolled loads of ZIP-type with $\gamma_n^P = \eta_n^P = \gamma_n^Q = \eta_n^Q = 0$ and $\xi_n^P = \xi_n^Q = 1$;

and results are reported, respectively, in Tables 8–10. In all the cases, it can be stated that PM assures higher accuracy than JM, with the only exception of the maximum error on P in the case 2.

In conclusion, looking at Tables 3–10, the improvement assured by PM in terms of accuracy is evident. It is due to the linearized model which, taking advantage of the radial topology of the distribution networks, adopts the square voltage amplitude variation as a variable. In this way, the inaccuracy introduced by linearization is reduced with respect to the classical JM. The improvement is more evident when DERs are equipped with a PQ control (f.i. see cases 1 and 3 for the 24-nodes network) and less evident when DERs are equipped with PV control (f.i. see case 4 for the 24-nodes network), since in this latter case the voltage amplitudes are imposed.

Table 8
Errors for the 237-nodes network: case 1.

	Average error [10^{-3} p.u.]			Maximum error [10^{-3} p.u.]		
	P	Q	V	P	Q	V
PM	0.0700	0.0129	0.2869	2.1470	0.4515	1.9665
JM	0.1518	0.0813	0.4958	2.2000	1.4608	4.2183

Table 9
Errors for the 237-nodes network: case 2.

	Average error [10^{-3} p.u.]			Maximum error [10^{-3} p.u.]		
	P	Q	V	P	Q	V
PM	0.0730	0.1971	0.3520	2.1272	7.1100	0.5614
JM	0.1257	0.3316	0.4757	1.9213	10.9870	0.8049

Table 10
Errors for the 237-nodes network: case 3.

	Average error [10^{-3} p.u.]			Maximum error [10^{-3} p.u.]		
	P	Q	V	P	Q	V
PM	0.0577	0.0085	0.2321	1.7684	0.3435	1.5599
JM	0.1296	0.0706	0.4219	1.8155	1.2338	3.5001

4.2. Application to sensitivity analysis: computational times

The PM is compared in terms of computational times with two sensitivity-based methods: the classical Jacobian method (JM) and a perturb and observe method (POM), based on a load-flow performed by MATPOWER (MP) [27]. Computational times are evaluated referring to the computing of sensitivity coefficients using MATLAB environment. Table 11 reports the computational times of PM, JM and POM for both the 24-nodes and 237-nodes networks. It is apparent that the computational times of PM are smaller than JM and POM; furthermore POM presents the worst performance.

For each method, the relationship between the increase of the computational times with respect to the increase of network dimension can be deduced by introducing the ratio between the numbers of the nodes r_N and the ratio between the computational times r_{CT} of, respectively, the 237-nodes and the 24-nodes network. Table 12 reports the values of r_N and r_{CT} for the PM, JM and POM. Looking at Table 12, it can be deduced that:

$$r_{CT} \simeq r_N \text{ for PM, } r_{CT} \simeq r_N^{1.31} \text{ for JM, } r_{CT} \simeq r_N^{1.64} \text{ for POM,}$$

that gives evidence that the larger the network, the higher the benefit

Table 11
Computational times for 24-nodes and 237-nodes networks.

Network	Computational time [s]		
	PM	JM	POM
24-nodes	0.087	0.099	2.115
237-nodes	0.872	2.087	95.613

Table 12
Increases of network dimension and computational times.

Ratio [p.u.]	PM	JM	POM
r_N	10.26	10.26	10.26
r_{CT}	10.02	21.08	45.21

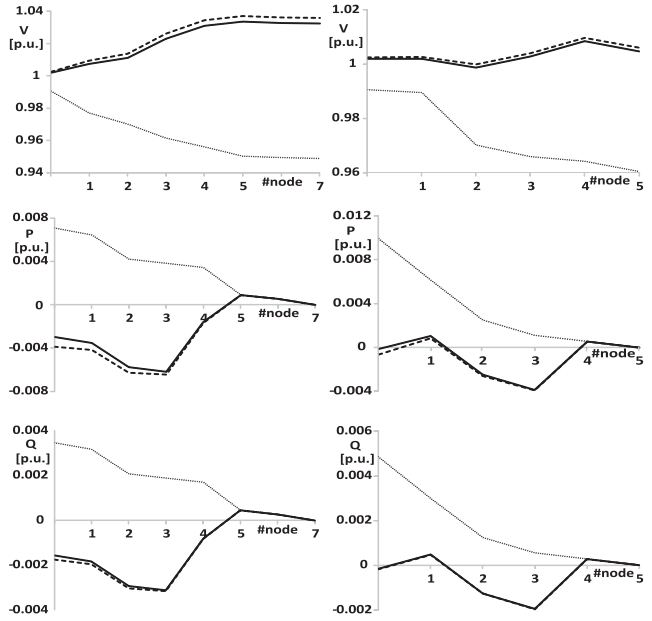

Fig. 6. Case A – Voltage, active and reactive power flows along the mains of feeder 1 (left) and 2 (right): initial point without DER by MP (dotted) and final point with DERs injection by MP (solid) and by PM (dashed).

assured by the PM. In conclusion, the high computational efficiency of the PM is related to the adoption of the closed-form solution, that avoids large matrix inversion or linear system solution.

4.3. Application to the load flow problem

The aim of this subsection is to show the use of the PM as alternative to non linear load-flow solution. Let the 24-nodes network be considered. The initial point refers to the operating conditions without DERs. Firstly, the PM is applied to evaluate the variations of the electrical variables caused by DER powers in the cases 3 and 4 of Section 4.1.1; then, the final values of the electrical variables are derived and compared with the non linear load flow solution, evaluated by MP. Figs. 6 and 7 report the electrical variables V_n,P_n,Q_n at each node along the two mains for the cases 3 and 4, respectively. Dotted plot refers to the initial point without DER injections; solid and dashed plots refer to the final operating condition obtained by respectively MP and PM. Analyzing Figs. 6 and 7 it is apparent that the PM is able to track the large variations of the electrical variables due to DER power injections. In particular referring to Fig. 7, it is evident that the model adopted by

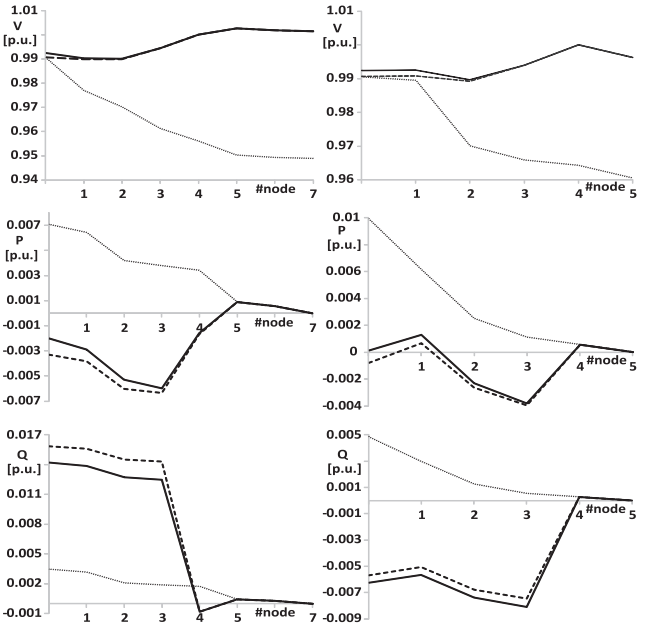

Fig. 7. Case B – Voltage, active and reactive power flows along the mains of feeder 1 (left) and 2 (right): initial point without DER by MP (dotted) and final point with DERs injection by MP (solid) and by PM (dashed).

the PM for DERs of PV-type accurately accounts for the variations of the voltage profile; in this case, errors are concentrated on active and reactive powers.

5. Conclusion

A linear method for the steady-state analysis of radial distribution systems with distributed energy resources has been proposed.

The method adopts a Jacobian-based model of the distribution system with a new set of variables, which is introduced to limit the approximation caused by system equation linearization. The proposed model is analytically solved by imposing border constraints and coupling equations for the radial topology, so as to obtain the closed-form expressions of the sensitivity coefficients.

The impact of distributed energy resources has been taken into account and, as a first step, only balanced operating condition have been considered. Future work will include also the changes in the operating conditions of the upstream supplying system and the actions of voltage regulators, such as tap-changers and capacitor banks, and will extend the proposed method to unbalanced distribution system operation.

Case studies have evidenced the good performance of the proposed method in terms of accuracy of the results and of computational efficiency of the algorithm with respect to other linear methods. Also the effectiveness of the proposed method in modeling the impact of different types of distributed energy resources on the network operation has been verified and compared with the classical non linear load flow solution.

Appendix A

For simplicity, the linearized model of the LNC in Fig. 3 is developed adopting the original numeration of the nodes of the network. Nomenclature for the LNC model and the expression of Jacobian matrices are reported in Tables 13 and 14, respectively.

Concerning the line, by linearizing (2):

$$\Delta \boldsymbol{x}_n^{out} = \mathbf{J}_n^{series}|_0 \Delta \boldsymbol{x}_n^{in} \tag{21}$$

Furthermore, by expressing (3) and (4) as variation, it results:

$$\Delta \boldsymbol{x}_n^{in} = \mathbf{S}_n \Delta \boldsymbol{x}_{n-1} \tag{22}$$

Table 13
Nomenclature for the LNC model.

$\boldsymbol{x}_n^{in} = (P_n^{in}, Q_n^{in}, V_{n-1}^2)^T$	Variables at the node A_n.
$\boldsymbol{x}_n^{out} = (P_n^{out}, Q_n^{out}, V_n^2)^T$	Variables at the node A'_n.
$\boldsymbol{x}_n^{line} = (P_n^{line}, Q_n^{line}, V_n^2)^T$	Variables outflowing the line.
$\boldsymbol{x}_n^{load} = (P_n^{load}, Q_n^{load}, 0)^T$	Variables for uncontrolled load.
$\boldsymbol{x}_n^{der} = (P_n^{der}, Q_n^{der}, 0)^T$	Variables for DER.
$\boldsymbol{x}_n^{lat} = (P_n^{lat}, Q_n^{lat}, 0)^T$	Variables for lateral.
$\mathbf{J}_n^{series}\|_0$	Jacobian matrix for line series components.
$\mathbf{J}_n^{line}\|_0$	Jacobian matrix for line.
$\mathbf{J}_n^{load}\|_0, \mathbf{J}_n^{load_1}\|_0, \mathbf{J}_n^{load_2}\|_0$	Jacobian matrices for uncontrolled load.
$\mathbf{J}_n^{der}\|_0, \mathbf{J}_n^{der_1}\|_0, \mathbf{J}_n^{der_2}\|_0$	Jacobian matrices for DER with P-V control.
$\mathbf{J}_n, \overline{\mathbf{J}}_n$	Jacobian matrices for LNC model.

Table 14
Expressions of matrices for LNC model.

$\mathbf{S}_n$	$\mathbf{J}_n^{load}\|_0$	$\mathbf{J}_n^{load_1}\|_0$	$\mathbf{J}_n^{load_2}\|_0$
$\begin{pmatrix} 1 & 0 & G_n/2 \\ 0 & 1 & -B_n/2 \\ 0 & 0 & 1 \end{pmatrix}$	$\begin{pmatrix} \frac{\partial P_n^{load}}{\partial \overline{P}_n^{load}}\|_0 & 0 & \frac{\partial P_n^{load}}{\partial V_n^2}\|_0 \\ 0 & \frac{\partial Q_n^{load}}{\partial \overline{Q}_n^{load}}\|_0 & \frac{\partial Q_n^{load}}{\partial V_n^2}\|_0 \\ 0 & 0 & 0 \end{pmatrix}$	$\begin{pmatrix} \frac{\partial P_n^{load}}{\partial \overline{P}_n^{load}}\|_0 & 0 & 0 \\ 0 & \frac{\partial Q_n^{load}}{\partial \overline{Q}_n^{load}}\|_0 & 0 \\ 0 & 0 & 0 \end{pmatrix}$	$\begin{pmatrix} 0 & 0 & \frac{\partial P_n^{load}}{\partial V_n^2}\|_0 \\ 0 & 0 & \frac{\partial Q_n^{load}}{\partial V_n^2}\|_0 \\ 0 & 0 & 0 \end{pmatrix}$

$\mathbf{J}_n^{der}\|_0$	$\mathbf{J}_n^{der_1}\|_0$	$\mathbf{J}_n^{der_2}\|_0$
$\begin{pmatrix} 1 & 0 & 0 \\ \frac{\partial Q_n^{der}}{\partial \overline{P}_{\overline{n}}^{der}}\|_0 & \frac{\partial Q_n^{der}}{\partial Q_{\overline{n}}^{der}}\|_0 & \frac{\partial Q_n^{der}}{\partial \overline{V}_{\overline{n}}^{2\,der}}\|_0 \\ \frac{\partial V_n^2}{\partial \overline{P}_{\overline{n}}^{der}}\|_0 & \frac{\partial V_n^2}{\partial Q_{\overline{n}}^{der}}\|_0 & \frac{\partial V_n^2}{\partial \overline{V}_{\overline{n}}^{2\,der}}\|_0 \end{pmatrix}$	$\begin{pmatrix} 1 & 0 & 0 \\ \frac{\partial Q_n^{der}}{\partial \overline{P}_{\overline{n}}^{der}}\|_0 - \frac{\frac{\partial Q_n^{der}}{\partial Q_{\overline{n}}^{der}}\|_0 \frac{\partial V_n^2}{\partial \overline{P}_{\overline{n}}^{der}}\|_0}{\frac{\partial V_n^2}{\partial Q_{\overline{n}}^{der}}\|_0} & 0 & \frac{\partial Q_n^{der}}{\partial \overline{V}_{\overline{n}}^{2\,der}} - \frac{\frac{\partial Q_n^{der}}{\partial Q_{\overline{n}}^{der}}\|_0 \frac{\partial V_n^2}{\partial \overline{V}_{\overline{n}}^{2\,der}}\|_0}{\frac{\partial V_n^2}{\partial Q_{\overline{n}}^{der}}\|_0} \\ 0 & 0 & 0 \end{pmatrix}$	$\begin{pmatrix} 0 & 0 & 0 \\ 0 & 0 & \frac{\partial Q_n^{der}}{\partial Q_{\overline{n}}^{der}}\|_0 \\ & & \frac{\partial V_n^2}{\partial Q_{\overline{n}}^{der}}\|_0 \\ 0 & 0 & 0 \end{pmatrix}$

$$\Delta \boldsymbol{x}_n^{line} = \mathbf{S}_n \Delta \boldsymbol{x}_n^{out} \tag{23}$$

where $\mathbf{S}_n$ is defined in Table 14. Finally, substituting (21) for $\Delta \boldsymbol{x}_n^{out}$ in (23) and (22) for $\Delta \boldsymbol{x}_n^{in}$ in the resulting equation, it is obtained:

$$\Delta \boldsymbol{x}_n^{line} = \mathbf{J}_n^{line}\|_0 \Delta \boldsymbol{x}_{n-1} \tag{24}$$

where $\mathbf{J}_n^{line}\|_0 = \mathbf{S}_n \mathbf{J}_n^{series}\|_0 \mathbf{S}_n$.

Concerning the node, by linearizing (5), it results:

$$\Delta \boldsymbol{x}_n^{load} = \mathbf{J}_n^{load}\|_0 (\Delta \overline{P}_n^{load}, \Delta \overline{Q}_n^{load}, \Delta V_n^2)^T \tag{25}$$

where $\mathbf{J}_n^{load}\|_0$ is defined in Table 14. The linearized model of uncontrolled loads is obtained by rewriting (25) as:

$$\Delta \boldsymbol{x}_n^{load} = \mathbf{J}_n^{load_1}\|_0 \Delta \overline{\mathbf{x}}_n^{load} + \mathbf{J}_n^{load_2}\|_0 \Delta \mathbf{x}_n \tag{26}$$

where $\mathbf{J}_n^{load_1}\|_0$ and $\mathbf{J}_n^{load_2}\|_0$ are defined in Table 14. Furthermore, according to (6) the linearized model of a DER with P-Q control is:

$$\Delta \boldsymbol{x}_n^{der} = \Delta \overline{\mathbf{x}}_n^{der} \tag{27}$$

In the case of a DER with P-V control, by linearizing (7), it results:

$$(\Delta P_n^{der}, \Delta Q_n^{der}, \Delta V_n^2)^T = \mathbf{J}_n^{der}\|_0 (\Delta \overline{P}_{\overline{n}}^{der}, \Delta Q_{\overline{n}}^{der}, \Delta \overline{V}_{\overline{n}}^2)^T \tag{28}$$

where $\mathbf{J}_n^{der}\|_0$ is the Jacobian matrix defined in Table 14. By substituting for $\Delta Q_{\overline{n}}^{der}$ the expression derived from the third row of (28) in the second row of (28), the linearized model of DER with P-V control is obtained:

$$\Delta \boldsymbol{x}_n^{der} = \mathbf{J}_n^{der_1}\|_0 \Delta \overline{\mathbf{x}}_{\overline{n}}^{der} + \mathbf{J}_n^{der_2}\|_0 \Delta \mathbf{x}_n \tag{29}$$

where $\mathbf{J}_n^{der_1}\|_0$ and $\mathbf{J}_n^{der_2}\|_0$ are defined in Table 14. Finally, from (8) the linearized model of the lateral is:

$$\Delta \boldsymbol{x}_n^{lat} = \Delta \widetilde{\mathbf{x}}_n^{lat} \tag{30}$$

Line and node models of the LNC are matched by balancing active and reactive powers at the node n according to:

$$\Delta \boldsymbol{x}_n = \Delta \boldsymbol{x}_n^{line} - \Delta \boldsymbol{x}_n^{load} + \Delta \boldsymbol{x}_n^{der} - \Delta \boldsymbol{x}_n^{lat} \tag{31}$$

By substituting in (31) for $\Delta \boldsymbol{x}_n^{line}$ (24), for $\Delta \boldsymbol{x}_n^{load}$ (26), for $\Delta \boldsymbol{x}_n^{der}$ the sum of (27) and (29),[2] and for $\Delta \boldsymbol{x}_n^{lat}$ (30), it is obtained:

$$\Delta \boldsymbol{x}_n = \bar{\mathbf{J}}_n \mathbf{J}_n^{line}|_0 \Delta \boldsymbol{x}_{n-1} + \bar{\mathbf{J}}_n(-\mathbf{J}_n^{load_1}|_0 \Delta \bar{\mathbf{x}}_n^{load} + \Delta \bar{\mathbf{x}}_n^{der} + \mathbf{J}_n^{der_1}|_0 \Delta \bar{\mathbf{x}}_{\bar{n}}^{der}) - \bar{\mathbf{J}}_n \Delta \tilde{\mathbf{x}}_n^{lat} \tag{32}$$

where

$$\bar{\mathbf{J}}_n \triangleq \left(\mathbf{I} + \mathbf{J}_n^{load_2}|_0 - \mathbf{J}_n^{der_2}|_0\right)^{-1} = (\mathbf{I} - \mathbf{J}_n^{load_2}|_0 + \mathbf{J}_n^{der_2}|_0)$$

Defining the vector of the variations of the injected powers $\Delta \bar{\mathbf{x}}_n^{inj}$ at the node n due to uncontrolled loads and DERs as:

$$\Delta \bar{\mathbf{x}}_n^{inj} \triangleq -\mathbf{J}_n^{load_1}|_0 \Delta \bar{\mathbf{x}}_n^{load} + \Delta \bar{\mathbf{x}}_n^{der} + \mathbf{J}_n^{der_1}|_0 \Delta \bar{\mathbf{x}}_{\bar{n}}^{der} \tag{33}$$

(32) is rewritten as:

$$\Delta \boldsymbol{x}_n = \mathbf{J}_n \Delta \boldsymbol{x}_{n-1} + \bar{\mathbf{J}}_n(\Delta \bar{\mathbf{x}}_n^{inj} - \Delta \tilde{\mathbf{x}}_n^{lat}) \tag{34}$$

where $\mathbf{J}_n = \bar{\mathbf{J}}_n \mathbf{J}_n^{line}|_0$. Eq. (34) is the model of the LNC, expressing the variation $\Delta \boldsymbol{x}_n$ as linear function of $\Delta \boldsymbol{x}_{n-1}$ and of assigned $\Delta \bar{\mathbf{x}}_n^{inj}$ and $\Delta \tilde{\mathbf{x}}_n^{lat}$.

Appendix B

B.1. LV network

By substituting (12) for $\Delta \tilde{\mathbf{x}}_{f,0,n_{fj}}^{lat}$ in (15), it results:

$$\begin{aligned}\Delta \boldsymbol{x}_{f,0,n} &= \sum_{k=1}^{N_{f_0}} \mathbf{A}_{f,0,n}(f,0,k) \Delta \bar{\mathbf{x}}_{f,0,k}^{inj} \\ &- \sum_{j=1}^{L_f} \mathbf{A}_{f,0,n}(f,0,n_{fj})(\Delta P_{f,j,0}, \Delta Q_{f,j,0}, 0)^{\mathrm{T}} + \mathbf{a}_{f,0,n} \Delta V_{LV}^2 \\ &\text{for } n = 0,\ldots,N_{f_0}\end{aligned} \tag{35}$$

By selecting the first and second row of (16) for $n = 0$ and adding a third row with zeros elements, it results:

$$(\Delta P_{f,\ell,0}, \Delta Q_{f,\ell,0}, 0)^{\mathrm{T}} = \sum_{k=1}^{N_{f\ell}} \mathbf{A}_{f,\ell,0}(f,\ell,k) \Delta \bar{\mathbf{x}}_{f,\ell,k}^{inj} + \bar{\mathbf{a}}_{f,\ell,0} \Delta V_{f,0,n_{f\ell}}^2 \tag{36}$$

where $\bar{\mathbf{a}}_{f,\ell,0}$ is equal to $\mathbf{a}_{f,\ell,0}$ in Table 1, expect for its third element which is set to zero. Substituting (36) in (35), it is obtained:

$$\begin{aligned}\Delta \boldsymbol{x}_{f,0,n} &= \sum_{k=1}^{N_{f_0}} \mathbf{A}_{f,0,n}(f,0,k) \Delta \bar{\mathbf{x}}_{f,0,k}^{inj} \\ &- \sum_{j=1}^{L_f} \sum_{k=1}^{N_{fj}} \mathbf{A}_{f,0,n}(f,0,n_{fj}) \mathbf{A}_{f,j,0}(f,j,k) \Delta \bar{\mathbf{x}}_{f,j,k}^{inj} \\ &- \sum_{j=1}^{L_f} \mathbf{A}_{f,0,n}(f,0,n_{fj}) \bar{\mathbf{a}}_{f,j,0} \Delta V_{f,0,n_{fj}}^2 + \mathbf{a}_{f,0,n} \Delta V_{LV}^2 \\ &\text{for } \quad n = 0,\ldots,N_{f_0}\end{aligned} \tag{37}$$

By selecting the third row of (37) for $n = n_{f\ell}$, it results:

$$\begin{aligned}\Delta V_{f,0,n_{f\ell}}^2 &= \sum_{k=1}^{N_{f_0}} \mathbf{b}_{f,0,n_{f\ell}}^{\mathrm{T}}(f,0,k) \Delta \bar{\mathbf{x}}_{f,0,k}^{inj} \\ &- \sum_{j=1}^{L_f} \sum_{k=1}^{N_{fj}} \mathbf{b}_{f,0,n_{f\ell}}^{\mathrm{T}}(f,0,n_{fj}) \mathbf{A}_{f,j,0}(f,j,k) \Delta \bar{\mathbf{x}}_{f,j,k}^{inj} \\ &- \sum_{j=1}^{L_f} \mathbf{b}_{f,0,n_{f\ell}}^{\mathrm{T}}(f,0,n_{fj}) \bar{\mathbf{a}}_{f,j,0} \Delta V_{f,0,n_{fj}}^2 + b_{f,0,n_{f\ell}} \Delta V_{LV}^2\end{aligned} \tag{38}$$

where $\mathbf{b}_{f,0,n_{f\ell}}^{\mathrm{T}}(f,0,n_{fj})$ is the 3^{th} row of $\mathbf{A}_{f,0,n_{f\ell}}(f,0,k)$ in Table 1 and $b_{f,0,n_{f\ell}}$ is the 3^{th} element of $\mathbf{a}_{f,0,n_{f\ell}}$ in Table 1. The set composed of (38) for $\ell = 1,\ldots,L_f$ is solved in the variables $\Delta V_{f,0,n_{f\ell}}^2$ yielding:

$$\begin{aligned}\Delta V_{f,0,n_{f\ell}}^2 &= \mathbf{e}_{f,\ell}^{\mathrm{T}} \sum_{k=1}^{N_{f_0}} \mathbf{D}_f(f,0,k) \Delta \bar{\mathbf{x}}_{f,0,k}^{inj} \\ &\mathbf{e}_{f,\ell}^{\mathrm{T}} \sum_{j=1}^{L_f} \sum_{k=1}^{N_{fj}} \mathbf{D}_f(f,0,n_{fj}) \mathbf{A}_{f,j,0}(f,j,k) \Delta \bar{\mathbf{x}}_{f,j,k}^{inj} \\ &+ \mathbf{e}_{f,\ell}^{\mathrm{T}} \mathbf{d}_f \Delta V_{LV}^2\end{aligned} \tag{39}$$

where $\mathbf{e}_{f,\ell}^{\mathrm{T}}$ is the ℓth row of $\mathbf{E}_f = (\mathbf{I} + \mathbf{C}_f)^{-1}$; matrices $\mathbf{C}_f, \mathbf{D}_f(f,0,k)$ and vectors $\mathbf{d}_f$ are defined in Table 15. Substituting (39) in (16) and (37) for

[2] The general case of connecting both a DER with PQ control and an other DER with PV control is considered.

Table 15
Expressions of vectors and matrices for LV network.

$\mathbf{C}_f$	$\mathbf{D}_f(f,0,k)$	$\mathbf{d}_f$
$(\mathbf{D}_f(f,0,n_{f_1})\overline{\mathbf{a}}_{f,1,0},\ldots,\mathbf{D}_f(f,0,n_{f_{L_f}})\overline{\mathbf{a}}_{f,L_f,0})$	$(\mathbf{b}^{\mathrm{T}}_{f,0,n_{f_1}}(f,0,k),\ldots,\mathbf{b}^{\mathrm{T}}_{f,0,n_{f_{L_f}}}(f,0,k))^{\mathrm{T}}$	$(b_{f,0,n_{f_1}},\ldots,b_{f,0,n_{f_{L_f}}})^{\mathrm{T}}$
$\mathbf{U}_{f,0,n}(f,j,k)$	$\mathbf{u}_{f,0,n}$	$\mathbf{G}_{f,0,n}$
	$\mathbf{A}_{f,0,n}(f,0,k)-\mathbf{G}_{f,0,n}\mathbf{D}_f(f,0,k)\ j=0$ $\mathbf{G}_{f,0,n}\mathbf{D}_f(f,0,n_{f_j})\mathbf{A}_{f,j,0}(f,j,k)-\mathbf{A}_{f,0,n}(f,0,n_{f_j})\mathbf{A}_{f,j,0}(f,j,k)\ j\neq 0$ $-\mathbf{G}_{f,0,n}\mathbf{d}_f+\mathbf{a}_{f,0,n}$ $\sum_{j=1}^{L_f}\mathbf{A}_{f,0,n}(f,0,n_{f_j})\overline{\mathbf{a}}_{f,j,0}\mathbf{e}^{\mathrm{T}}_{f,j}$	
$\mathbf{U}_{f,\ell,n}(f,j,k)$		$\mathbf{u}_{f,\ell,n}$
	$\mathbf{a}_{f,\ell,n}\mathbf{e}^{\mathrm{T}}_{f,\ell}\mathbf{D}_f(f,0,k)\ j=0$ $\mathbf{A}_{f,\ell,n}(f,\ell,k)-\mathbf{a}_{f,\ell,n}\mathbf{e}^{\mathrm{T}}_{f,\ell}\mathbf{D}_f(f,0,n_{f_\ell})\mathbf{A}_{f,\ell,0}(f,\ell,k)\ j=\ell$ $-\mathbf{a}_{f,\ell,n}\mathbf{e}^{\mathrm{T}}_{f,\ell}\mathbf{D}_f(f,0,n_{f_j})\mathbf{A}_{f,j,0}(f,j,k)\ j\neq 0,\ell$ $\mathbf{a}_{f,\ell,n}\mathbf{e}^{\mathrm{T}}_{f,\ell}\mathbf{d}_f$	

Table 16
Expressions of vectors and matrices for distribution system.

$\mathbf{w}$	α	β	$\mathbf{T}_{f,\ell,n}(i,j,k)$
$-(j^{ss}_{31}j^{ss}_{32},0)^{\mathrm{T}}/j^{ss}_{33}$	$\mathbf{w}/\beta$	$1-\mathbf{w}^{\mathrm{T}}\sum_{i=1}^{F}\mathbf{u}_{i,0,0}$	$\mathbf{U}_{f,\ell,n}(i,j,k)+\mathbf{u}_{f,\ell,n}\boldsymbol{\alpha}^{\mathrm{T}}\mathbf{U}_{i,0,0}(i,j,k)\ i=f$ $\mathbf{u}_{f,\ell,n}\boldsymbol{\alpha}^{\mathrm{T}}\mathbf{U}_{i,0,0}(i,j,k)\ i\neq f$

$f=1,\ldots,F$, it is obtained:

$$\Delta\boldsymbol{x}_{f,\ell,n}=\sum_{j=0}^{L_f}\sum_{k=1}^{N_{fj}}\mathbf{U}_{f,\ell,n}(f,j,k)\Delta\overline{\mathbf{x}}^{inj}_{f,j,k}+\mathbf{u}_{f,\ell,n}\Delta V^2_{LV}$$
$$\text{for } f=1,\ldots,F,\ \ell=0,\ldots,L_f\quad n=0,\ldots,N_{f_\ell} \tag{40}$$

where $\mathbf{U}_{f,\ell,n}(f,j,k)$ and $\mathbf{u}_{f,\ell,n}$ are defined in Table 15. Eq. (40) is the model of the LV network, expressing the variation $\Delta\boldsymbol{x}_{f,\ell,n}$ as linear function of assigned $\Delta\overline{\mathbf{x}}^{inj}_{f,j,k}$ and ΔV^2_{LV}.

B.2. Distribution system

Substituting (13) in (9), it is obtained:

$$\Delta\boldsymbol{x}_{MV}=\mathbf{J}^{ss}|_0\left(\sum_{i=1}^{F}\Delta P_{i,0,0},\sum_{i=1}^{F}\Delta Q_{i,0,0},\Delta V^2_{LV}\right)^{\mathrm{T}} \tag{41}$$

The third row of (41) can be written as:

$$0=(j^{ss}_{31},j^{ss}_{32},0)\sum_{i=1}^{F}\Delta\boldsymbol{x}_{i,0,0}+j^{ss}_{33}\Delta V^2_{LV} \tag{42}$$

Solving (42) in ΔV^2_{LV} it yields:

$$\Delta V^2_{LV}=\mathbf{w}^{\mathrm{T}}\sum_{i=1}^{F}\Delta\boldsymbol{x}_{i,0,0} \tag{43}$$

where $\mathbf{w}$ is defined in Table 16. Let (17) be particularized with $f=i,\ell=0,n=0$ and substituted for $\Delta\boldsymbol{x}_{i,0,0}$ in (43); the resulting equation is solved with respect to ΔV^2_{LV} yielding:

$$\Delta V^2_{LV}=\sum_{i=1}^{F}\sum_{j=0}^{L_i}\sum_{k=1}^{N_{ij}}\boldsymbol{\alpha}^{\mathrm{T}}\mathbf{U}_{i,0,0}(i,j,k)\Delta\overline{\mathbf{x}}^{inj}_{i,j,k} \tag{44}$$

where $\boldsymbol{\alpha}$ is defined in Table 16. Eventually, by substituting (44) into (17), it yields:

$$\Delta \boldsymbol{x}_{f,\ell,n} = \sum_{i=1}^{F} \sum_{j=0}^{L_i} \sum_{k=1}^{N_{fj}} \mathbf{T}_{f,\ell,n}(i,j,k) \Delta \bar{\mathbf{x}}_{i,j,k}^{inj}$$
$$\text{for } f = 1,\ldots,F \quad \ell = 0,\ldots,L_f \quad n = 0,\ldots,N_{f\ell} \tag{45}$$

where $\mathbf{T}_{f,\ell,n}(i,j,k)$ is defined in Table 16. Eq. (45) is the model of the LV distribution system, expressing the variation $\Delta \boldsymbol{x}_{f,\ell,n}$ as linear function of assigned $\Delta \bar{\mathbf{x}}_{f,j,k}^{inj}$.

References

[1] Martí J, Ahmadi H, Bashualdo L. Linear power-flow formulation based on a voltage-dependent load model. IEEE Trans Power Deliv 2013;28(3):1682–90.
[2] Garces A. A linear three-phase load flow for power distribution systems. IEEE Trans Power Syst 2015;31(1):827–8.
[3] Wang Y, Zhang N, Li H, Yang J, Kang C. Linear three-phase power flow for unbalanced active distribution networks with pv nodes. CSEE J Power Energy Syst 2017;3(3):321–4.
[4] O'Connell A, Flynn D, Keane A. Rolling multi-period optimization to control electric vehicle charging in distribution networks. IEEE Trans Power Syst 2014;29(1):340–8.
[5] Ahmadi H, Martí J. Distribution system optimization based on a linear power-flow formulation. IEEE Trans Power Deliv 2015;30(1):25–33.
[6] Ayres HM, Salles D, Freitas W. A practical second-order based method for power losses estimation in distribution systems with distributed generation. IEEE Trans Power Syst 2014;29(2):666–74.
[7] Jothibasu S, Santoso S. Sensitivity analysis of photovoltaic hosting capacity of distribution circuits. In: IEEE power and energy society general meeting (PESGM); 2016. p. 1–5.
[8] Sathyanarayana BR, Heydt GT. Sensitivity-based pricing and optimal storage utilization in distribution systems. IEEE Trans Power Deliv 2013;28(2):1073–82.
[9] Tamp F, Ciufo P. A sensitivity analysis toolkit for the simplification of mv distribution network voltage management. IEEE Trans Smart Grid 2014;5(2):559–68.
[10] Džafić I, Jabr R, Halilovic E, Pal B. A sensitivity approach to model local voltage controllers in distribution networks. IEEE Trans Power Syst 2014;29(3):1419–28.
[11] Brenna M, De Berardinis E, Delli Carpini L, Foiadelli F, Paulon P, Petroni P, et al. Automatic distributed voltage control algorithm in smart grids applications. IEEE Trans Smart Grid 2013;4(2):877–84.
[12] Kersting W. Distribution system modeling and analysis. 3rd ed. CRC Press, Taylor and Francis Group; 2012.
[13] Weckx S, D'Hulst R, Driesen J. Voltage sensitivity analysis of a laboratory distribution grid with incomplete data. IEEE Trans Smart Grid 2015;6(3):1271–80.
[14] Mugnier C, Christikou K, Jaton J, De Vivo M, Carpita M, Paolone M. Model-less/measurement-based computation of voltage sensitivities in unbalanced electrical distribution networks. In: IEEE power systems computation conference (PSCC); Jun. 2016. p. 1–7.
[15] Christakou K, LeBoudec J-Y, Paolone M, Tomozei D-C. Efficient computation of sensitivity coefficients of node voltages and line currents in unbalanced radial electrical distribution networks. IEEE Trans Smart Grid 2013;4(2):741–50.
[16] Kathod D, Pant V, Sharma J. A novel approach for sensitivity calculations in the radial distribution system. IEEE Trans Power Deliv 2006;21(4):2048–57.
[17] Zhou Q, Bialek JW. Simplified calculation of voltage and loss sensitivity factors in distribution networks. In: Power systems computation conference (PSCC); Jul. 2008. p. 1–6.
[18] Bolognani S, Zampieri S. On the existence and linear approximation of the power flow solution in power distribution networks. IEEE Trans Power Syst 2016;31(1):163–72.
[19] Youssef KH. A new method for online sensitivity-based distributed voltage control and short circuit analysis of unbalanced distribution feeders. IEEE Trans Smart Grid 2015;6(3):1253–60.
[20] Gurram R, Subramanyam B. Sensitivity analysis of radial distribution network–adjoint network method. Int J Elect Power Energy Syst 1999;21(5):323–6.
[21] Baran M, Wu F. Optimal sizing of capacitors placed on a radial distribution system. IEEE Trans Power Deliv 1989;4(1):735–43.
[22] Di Fazio AR, Russo M, Valeri S, De Santis M. Sensitivity-based model of low voltage distribution systems with distributed energy resources. Energies 2016;9. < http://www.mdpi.com/1996-1073/9/10/801 > .
[23] Bokhari A, Alkan A, Dogan R, Diaz-Aguiló M, de León F, Czarkowski D, et al. Experimental determination of the zip coefficients for modern residential, commercial, and industrial loads. IEEE Trans Power Deliv 2014;29(3):1372–81.
[24] Adhikari S, Li F, Li H. P-q and p-v control of photovoltaic generators in distribution systems. IEEE Trans Smart Grid 2015;6(6):2929–41.
[25] Di Fazio AR, Fusco G, Russo M. Smart der control for minimizing power losses in distribution feeders. Electr Power Syst Res 2014;109:71–9.
[26] Available: http://ewh.ieee.org/soc/pes/dsacom/testfeeders/index.html.
[27] Zimmerman RD, Murillo-Sánchez CE, Thomas RJ. MATPOWER: steady-state operations, planning and analysis tools for power systems research and education. IEEE Trans Power Syst 2011;26(1):1–19 Available: <http://www.pserc.cornell.edu//matpower/> .